

# On Three-Electron Bonds and Hydrogen Bonds in the Open-Shell Complexes $[\text{H}_2\text{X}_2]^+$ for $\text{X} = \text{F}, \text{Cl}, \text{and Br}^\dagger$

Andrzej Bil,\* Sławomir Berski, and Zdzisław Latajka

Faculty of Chemistry, University of Wrocław, Joliot-Curie 14, 50-383 Wrocław, Poland

Received August 15, 2006

The  $[\text{H}_2\text{X}_2]^+$  ( $\text{X} = \text{Cl}, \text{Br}$ ) formula could refer to two possible stable structures, namely, the hydrogen-bonded complex and the three-electron-bonded one. In contrary to the results published by other authors, we claim that for the F-type structures the hydrogen-bonded form is the only possible one and the  $[\text{HFFH}]^+$  complex is an artifact as its wave function is unstable. For all analyzed molecules, the IR anharmonic spectra have been simulated, which enabled a deeper analysis of other authors' published results of IR low-temperature matrix experiments. Topological atoms in molecules and electron localization function investigations have revealed that the nature of the bond in three-electron-bonded structures is similar to the covalent-depleted one in  $\text{F}_2$  or  $\text{HOO}$  molecules, but the effect of removing electrons from the bond area is stronger.

## INTRODUCTION

Considering weak or medium intermolecular hydrogen bonds, we usually think of structures in which the existence of such interactions marginally influence the geometrical parameters of interacting subsystems. These interactions are considered as mostly of electrostatic origin. In the case of strong hydrogen bonds, a covalent character of intermolecular interaction dominates.<sup>1</sup> Other weak intermolecular interactions are considered as mostly electrostatic.

A three-electron-bonded system is defined as one in which a bonding  $\sigma$  molecular orbital centered on the two neighboring atoms in a molecule is doubly occupied whereas the complementary  $\sigma^*$  antibonding one is singly occupied.<sup>2</sup> Therefore, for the mentioned bond, the formal bond order is 0.5.

The stable structures containing two-center three-electron bonds are a subject of both experimental and theoretical scrutiny. For example, the structures of the type  $[\text{H}_2\text{X}_2]^+$ ,  $\text{X} = \text{F}, \text{Cl}, \text{Br}, \text{I}, \text{and At}$ , were put to investigations encompassing an analysis of potential energy surface (PES) and examination of the influence of relativistic effects on the properties of the complexes containing the heaviest  $\text{X}$  atoms.<sup>2–4</sup> It was revealed that there were two different structures referring to local minima on the PES, namely, the one with a hydrogen bond and the other three-electron-bonded (Figure 1). The three-electron bond was also investigated in other chemical systems.<sup>5–11</sup>

$[\text{H}_2\text{Cl}_2]^+$  and  $[\text{H}_2\text{Br}_2]^+$  complexes were stable in a low-temperature neon matrix,<sup>12,13</sup> which enabled obtaining of their IR spectra. The authors of the papers did not discuss the structures of examined complexes in the context of the obtained spectra. They assumed the three-electron-bonded structure of these complexes on the basis of the earlier theoretical investigations of the PESs of such structures.<sup>2,3</sup>

In this work, the open-shell  $[\text{H}_2\text{X}_2]^+$  systems for  $\text{X} = \text{F}, \text{Cl}, \text{and Br}$  have been investigated using theoretical ab initio

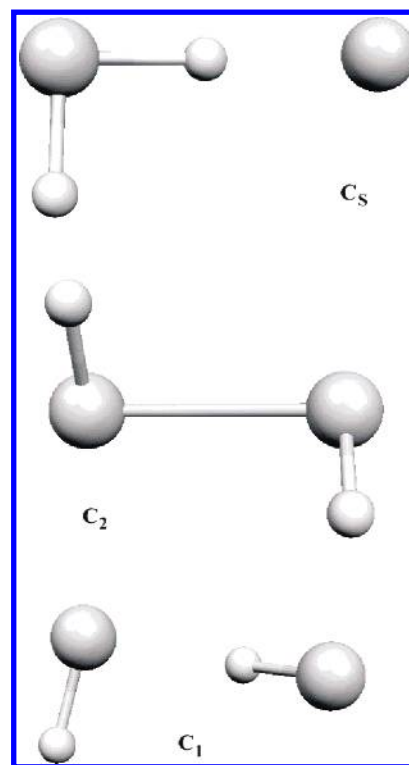


**Figure 1.** Structures of the  $[\text{HXH}\cdots\text{X}]^+$ ,  $[\text{HXXH}]^+$ , and TS complexes.

as well as topological methods. The paper is devoted to three main aims. First of all, we would like to summarize the facts about the PESs of these structures, as in our opinion there are some doubts when it comes to the results reported in the previous papers, especially in the case of fluorine-containing complexes. The next aim is to simulate harmonic as well as anharmonic IR spectra of these complexes, as they have not been reported as of yet. In the context of the calculated spectra as well as the shape of the PES, some results and conclusions from the experimental papers<sup>12,13</sup> are discussed, especially an assignment of certain observed bands. The last

<sup>†</sup> This publication is dedicated to the memory of Professor Jan Mozrzymas.

\* Corresponding author e-mail: abil@elrond.chem.uni.wroc.pl.

aim, to which the largest part of this paper is devoted, is to characterize the intermolecular interactions in all possible  $[\text{H}_2\text{X}_2]^+$  complexes on the basis of information available from the topological analyses of a computed electron density using the atoms in molecule (AIM) approach<sup>14</sup> as well as the electron localization function (ELF) method.<sup>15,16</sup> The results have been supported with the description given by natural bond order (NBO) analysis.<sup>17</sup>

The last of the mentioned above issues is especially interesting. The  $[\text{HXXH}]^+$  complexes are of particular importance, being small models of the systems with 2c–3e bonds. An in-depth analysis of the nature of the bond in these model systems using a variety of methods is especially valuable as it provides information about the whole class of molecules containing such a bond.

Making conclusions about the properties of molecular systems on the basis of an orbital approximation is disputable, though it is often performed and, in the case of systems well-described by Lewis structures, could be very useful. Although utilization of the total wave function obtained in the orbital approximation is methodologically correct, each of the orbitals considered separately has no physical meaning. The choice of the orbital form is, which is well-known, arbitrary and established by the choice of any unitary transformation of the wave function.

Methods such as AIM or ELF, although their usefulness in analyses of particular types of bonds could be disputable, have one unquestionable advantage over the methods which are based on the orbital approach. Namely, both the electron density and electron localization function are invariant under the unitary transformations of the wave function and, therefore, are free from nonphysical effects resulting from an arbitrary choice of molecular orbitals. Moreover, these methods allow calculation of some parameters by means of which one can quantitatively compare properties of bonds of any type.

For example, when some local properties of hydrogen bonds in  $[\text{HBrH}\cdots\text{Br}]^+$  and  $[\text{HFH}\cdots\text{F}]^+$  complexes obtained by means of AIM and ELF methods were compared, it occurred that, in the first case, the bond is mostly covalent whereas, in the case of an F-type complex, the closed-shell character dominates. This conclusion is important as, because of the fundamental reasons, it is not possible to perform the interaction energy decomposition and determine electrostatic shares in the case of charged complexes.

Although there is constant discussion between Bader and opponents about the AIM method,<sup>18–21</sup> we decided to apply it in investigations of  $[\text{H}_2\text{X}_2]^+$  systems. Our experience with topological methods as well as acres of publications by many authors lets us consider the AIM and ELF methods as valuable tools to investigate the nature of bonding in molecules, complexes, and solids.

## COMPUTATIONAL METHODOLOGY

In the paper,<sup>2</sup> it was proved that the 6-31g\* basis set suffices for the geometry optimization of structures with an intermolecular hydrogen bond with first and second row atoms and their three-electron-bonded isomers. The total energy of the systems was obtained as a single-point calculation in the TZV basis set with the polarization functions for geometry optimized at the 6-31g\* level. The

influence of diffuse functions on the results was emphasized. For the examined systems, an electron correlation is well-described by second-order Möller–Plesset perturbation theory.<sup>22</sup>

On the other hand, the 6-311++g(2d,2p)<sup>23–25</sup> basis set is recommended as the smallest one which still suffices to reach topological stability with respect to the basis set variation for L-graphs in the Laplacian of electron density.<sup>26</sup>

In this work, for  $[\text{H}_2\text{F}_2]^+$  and  $[\text{H}_2\text{Cl}_2]^+$  systems, all calculations have been performed at the MP2(Full)/6-311++g(2d,2p) 6D level of calculation and at the MP2(Full)/6-311++g(3df,2pd) 6D 10F level for the remaining Br-type compounds. As a starting point in geometry optimization, the geometrical parameters of all analyzed structures have been taken from the paper.<sup>4</sup> Geometry optimizations, calculations of IR spectra, and NBO analysis have been performed using the Gaussian 03<sup>27</sup> and GAMESS<sup>28</sup> programs.

For all calculated systems, a spin contamination is small, which confirms that a single-determinant approach is sufficient for the correct description of the analyzed molecules. The largest value of  $\langle S^2 \rangle$  was in the case of the  $[\text{HBrBrH}]^+$  complex and amounted to 0.7715.

Calculations of the anharmonic frequencies have been carried out without any coupling between oscillation normal modes, as implemented in Gaussian 03. The intensities have been calculated for harmonic modes. AIM analyses have been executed by means of the AIMPAC packet,<sup>29</sup> whereas ELF calculations have been performed using TopMod software.<sup>30</sup> The graphical analysis of ELF pictures has been performed by means of the SciAn software.<sup>31</sup>

The above-mentioned topological analyses have been performed using a set of natural orbitals for the spin density (*pop*=*NaturalSpin density*=*all* keywords in Gaussian 03) generated with the same method and basis sets which have been used for geometry optimization. The 0.05 bohr mesh size has been used for the electron density integration.

Units which are used throughout this paper are as follows: distances in angstroms (Å), angles and torsion angles in degrees (°), energies in kilocalories per mole (kcal mol<sup>–1</sup>), IR frequencies in centimeters<sup>–1</sup> (cm<sup>–1</sup>), and IR intensities in kilometers per mole (km mol<sup>–1</sup>). Other dimensional values are in atomic units.

## RESULTS AND DISCUSSION

**PES Analyses and IR spectra.** Table 1 characterizes the chosen points on the PES of  $[\text{H}_2\text{X}_2]^+$  systems. The values of energy are expressed with respect to the arbitrary chosen level of reference, namely, the sum of the total energies of the free  $\text{H}_2\text{X}^+$  and  $\text{X}^*$  moieties. The table also contains results corrected for the zero-point energy (ZPE) effect calculated in the harmonic as well as anharmonic framework.

The shape of the PES of investigated systems obtained at the MP2(Full)/6-311++g(2d,2p) level for Cl-type structures and at the MP2(Full)/6-311++g(3df, 3pd) one for Br-type molecules is consistent with the previously reported data obtained by means of methods including electron correlation effects. Two local minima have been observed, namely, the hydrogen-bonded structure  $[\text{HXH}\cdots\text{X}]^+$  and the most stable  $[\text{HXXH}]^+$  three-electron-bonded one (Figure 1). The energy difference between these minima is about 7.8 kcal mol<sup>–1</sup> for Cl-type systems and about 9.1 kcal mol<sup>–1</sup> for Br-type

**Table 1.** Energies of the Investigated Systems in Relation to the Sum of Energies of  $\text{H}_2\text{X}^+$  and  $\text{X}^*$  Monomers

		$[\text{HX}\cdots\text{X}]^+$	TS	$[\text{HX}-\text{XH}]^+$	$\text{HX} + \text{HX}^+$
F	$E_{\text{tot}}^{a,b}$	-11.44/-11.64			37.61/37.61
	$E_{\text{tot}} + \text{ZPE}$	-10.49			35.85
	$E_{\text{tot}} + \text{ZPE}/\text{anh}$	-10.69			35.90
Cl	$E_{\text{tot}}$	-12.77/-13.07	-3.82/-5.93	-21.38/-20.42	11.08/10.90
	$E_{\text{tot}} + \text{ZPE}$	-12.92		-20.44	9.58
	$E_{\text{tot}} + \text{ZPE}/\text{anh}$	-13.06		-20.82	9.59
Br	$E_{\text{tot}}$	-15.03/-13.56	-7.53/-8.51	-25.03/-23.73	7.42/7.63
	$E_{\text{tot}} + \text{ZPE}$	-15.52		-24.69	6.07
	$E_{\text{tot}} + \text{ZPE}/\text{anh}$	-15.61		-24.69	6.11

<sup>a</sup> MP2(full). <sup>b</sup> CCSD-T(full)// MP2(full).**Table 2.** Geometrical Parameters of the Investigated Systems

	HX	$\text{HX}^+$	$[\text{HXH}\cdots\text{X}]^+$						$\text{H}_2\text{X}^+$	
	H-X	H-X	H-X	X-H	H...X	HXH	XHX	HXXH	H-X	HXH
F	0.918	0.998	0.952	1.017	1.409	114.16	174.60	180	0.961	112.16
Cl	1.270	1.310	1.291	1.444	1.752	95.16	177.36	180	1.301	94.07
Br	1.408	1.440	1.424	1.622	1.803	92.87	178.68	180	1.433	92.30

	$[\text{HXXH}]^+$				TS ( $\text{HX}-\text{H}'\text{X}'$ )						
	H-X	$\text{X}\cdots\text{X}$	HXX	HXXH	H-X	$\text{X}\cdots\text{X}'$	$\text{X}\cdots\text{H}'$	$\text{X}'-\text{H}'$	HXH'	XH'X'	HXH'X'
Cl	1.291	2.566	92.30	102.46	1.285	2.953	2.006	1.337	98.07	122.80	-94.57
Br	1.424	2.806	90.75	96.36	1.420	3.218	2.088	1.481	94.60	127.95	-93.20

ones. The energy barrier for an isomerization process is about 17.5 kcal mol<sup>-1</sup> for systems of both types. The transition structure (TS) between the local energy minimum complexes is also depicted in Figure 1. Geometrical parameters of all discussed molecules are collected in Table 2.

For all discussed above structures, single-point total energy calculations have been performed at the CCSD-T(Full) level using the same basis sets as in the MP2 calculations. As can be seen from Table 1, the PES has not been changed qualitatively. For F-type systems, the results are almost the same as those obtained at the MP2 level, which suggests that, for these structures containing the smallest number of electrons, the MP2 method seems to cover most of the dynamic correlation effects. In the case of heavier structures, the main effect of using the CCSD-T method is lowering the barrier of isomerization between three-electron-bonded and hydrogen-bonded structures.

The data presented in the table do not contain basis set superposition errors (BSSEs) because, if the properties of  $[\text{HXH}\cdots\text{X}]^+$  and  $[\text{HX}-\text{HX}]^+$  complexes are to be compared, the calculations for both hydrogen-bonded and three-electron-bonded structures should be performed in the same way. For the three-electron-bonded systems, where the bonding energy is large and the HX and  $\text{HX}^+$  moieties undergo a large deformation during a complex formation, it seems senseless to force BSSE corrections. The BSSEs calculated for  $[\text{HFH}\cdots\text{F}]^+$ ,  $[\text{HClH}\cdots\text{Cl}]^+$ , and  $[\text{HBrH}\cdots\text{Br}]^+$  at the MP2(full) level are 1.85, 2.54, and 0.89 kcal mol<sup>-1</sup>, respectively, which suggests that the used basis sets are large enough to ensure that BSSE does not influence strongly the shape of the PES.

Calculated ionization potentials for HBr and HCl molecules are 11.725 and 12.557 eV and show good conformity with experimental values [11.645 and 12.748(5) eV, respectively<sup>32</sup>]. The binding energy of the complex  $[\text{H}_2\text{Cl}_2]^+$  ( $[\text{H}_2-\text{Cl}_2]^+ \rightarrow \text{HCl} + \text{HCl}^+$ ) obtained from the results of the molecular beam photoionization experiment<sup>32</sup> is about 20-(2) kcal mol<sup>-1</sup> and differs from the value obtained in our

calculations. A similar situation is in the case of the Br-containing complex, the experimental binding energy of which is about 23(2) kcal mol<sup>-1</sup>. The obvious reason is that, in the photoionization experiment, the excitation process is adiabatic and preserves more or less the structure of the  $(\text{HX})_2$  van der Waals complex, which is more similar to the  $[\text{HXH}\cdots\text{X}]^+$  structure than to the equilibrium geometry of the  $[\text{HXXH}]^+$  complex.

Results completely different from the ones reported in previous papers<sup>2-4</sup> have been obtained in the investigation of PES of the F-containing structures. The papers reported the hydrogen-bonded  $[\text{HFH}\cdots\text{F}]^+$  structure as more stable than the  $[\text{HFFH}]^+$  one, which is also in the local minimum on the PES. Our calculation proved that the hydrogen-bonded complex is the only possible structure, and the three-electron-bonded one must be regarded as an artifact. Repeating the calculation reported in paper,<sup>4</sup> we have obtained the three-electron-bonded structure, the wave function of which was, however, unstable. It means that the wave function does not refer to the minimum of the average energy calculated in the set of determinants constructed from the Hartree-Fock orbitals obtained for the "equilibrium" geometry of the three-electron-bonded structure. The attempts consisting of altering the initial guess to find a stable wave function referring to this structure failed.

Calculation of the IR spectrum for such an "optimized" three-electron-bonded structure leads to completely improper results. The problem was spotted by Gill and Radom<sup>2</sup> where the ZPE correction for the three-electron-bonded structure was taken as the same as for the hydrogen-bonded one, but without any commentary on the reason for that. The authors must have encountered difficulties with the IR spectrum simulation for the  $[\text{HFFH}]^+$  structure but did not analyze them.

Interestingly, prior to the cited papers, the results of experimental investigations of such structures were reported,<sup>32</sup> which could suggest that three-electron-bonded

**Table 3.** Observed Bands for the Br- and Cl-Containing Molecules

	gas phase	Ne matrix
HCl	2906.25	2899.6
HCl <sup>+</sup>	2568.62	2543.8
H <sub>2</sub> Cl <sup>+</sup>	2643.22, 2630.14	2637.5, 2622.3
[H <sub>2</sub> Cl <sub>2</sub> ] <sup>+</sup>		2704.1, 2703.1
HBr	2558.54	2556.4
HBr <sup>+</sup>	2346.72	2355.7
[H <sub>2</sub> Br <sub>2</sub> ] <sup>+</sup>		2440.3

F-type complex did not exist. The authors obtained results for [H<sub>2</sub>Br<sub>2</sub>]<sup>+</sup> and [H<sub>2</sub>Cl<sub>2</sub>]<sup>+</sup> complexes, while there was no evidence for the [H<sub>2</sub>F<sub>2</sub>]<sup>+</sup> complex.

To sum up, contrary to the previously reported conclusions, we claim that the only possible equilibrium structure of the [H<sub>2</sub>F<sub>2</sub>]<sup>+</sup> complex is the hydrogen-bonded one.

In a previous experimental work,<sup>13</sup> the authors reported results of investigations of products obtained in the reaction in a Ne:HBr low-temperature matrix with co-deposited discharge-excited Ne atoms. Recorded IR frequencies were interpreted as coming from HBr, HBr<sup>+</sup>, and [H<sub>2</sub>Br<sub>2</sub>]<sup>+</sup> structures, but for the complex, no geometrical structure was suggested. No bands which could be interpreted as coming from the H<sub>2</sub>Br<sup>+</sup> ion were observed.

In light of the data in Table 1, there is no doubt that the most likely process is a formation of three-electron-bonded structures which are about 30.8 kcal mol<sup>-1</sup> more stable than reagents HX + HX<sup>+</sup>. Moreover, this process does not require breaking any bonds in monomers. In the matrix experiment, only one band (2440.3 cm<sup>-1</sup>) coming from the [H<sub>2</sub>Br<sub>2</sub>]<sup>+</sup> molecule was recognized and assigned to H–Br stretching vibration (Table 3). Corresponding calculated values (Table 4) are 2542.4 cm<sup>-1</sup> for the [HBrH⋯Br]<sup>+</sup> complex as well as 2537.7 cm<sup>-1</sup> and 2532.4 cm<sup>-1</sup> in the case of the three-electron-bonded structure. The values are similar; therefore, it is impossible to choose the proper structure on the basis of this frequency only. However, in the case of the three-electron-bonded structure, the H–Br asymmetric stretching band is of the largest intensity in the calculated spectrum. On the contrary, in the simulated spectrum of the hydrogen-bonded complex, there are two much more intense bands which should be observed experimentally if this complex exists in the matrix, namely, the H–Br stretching band in the Br–H–Br hydrogen bridge and the H–Br–H bending band. Calculated IR spectra together with the lack of these bands in the experimental spectrum confirm the presence of the three-electron-bonded structure in the matrix only.

A previous paper<sup>12</sup> was devoted to the experimental study of the Cl-containing species by the same method as in the case of Br-type molecules.<sup>13</sup> The IR bands originating from HCl, HCl<sup>+</sup>, and [H<sub>2</sub>Cl<sub>2</sub>]<sup>+</sup> molecules were recorded (Table 3). Moreover, after mercury-arc irradiation of the deposit in the matrix, weak absorptions at 2637.5 and 2622.3 cm<sup>-1</sup> were detected, which were assigned tentatively to the two stretching fundamentals of H<sub>2</sub>Cl<sup>+</sup>. As it was mentioned in the introduction, the authors assumed the three-electron-bonded structure of the [H<sub>2</sub>Cl<sub>2</sub>]<sup>+</sup> complex on the basis of the results reported in previous theoretical papers.

The shape of the PES of Cl-containing species (Table 1) confirms that, in the IR matrix experiment, the [HCiClH]<sup>+</sup> complex should be observed. In the case of HCl, HCl<sup>+</sup>, and H<sub>2</sub>Cl<sup>+</sup> molecules, the H–Cl calculated stretching frequencies

**Table 4.** Calculated IR Spectra (Anharmonic Frequencies, Harmonic Intensities)

Br		Cl		F		description
freq	int	freq	int	freq	int	
HX						
2660.6	17.0	2875.6	47.8	3990.6	123.7	stretching
HX <sup>+</sup>						
2445.9	184.3	2559.6	296.9	2963.7	589.5	stretching
H <sub>2</sub> X <sup>+</sup>						
2480.8	144.0	2634.8	217.5	3340.1	235.4	sym. str.
2473.6	212.0	2618.9	328.3	3335.7	869.0	asym. str.
1044.6	0.3	1236.1	20.7	1383.4	252.4	bending
[HXXH] <sup>+</sup>						
2537.7	83.2	2712.6	128.0			HX sym str.
2532.4	165.2	2709.4	232.4			HX asym str.
417.1	0.2	491.6	0.0			HXX sym. bend.
413.1	49.2	486.0	110.7			HXX asym. bend.
171.9 <sup>a</sup>	20.4	273.7 <sup>b</sup>	0.1			
167.8 <sup>a</sup>	10.9	175.9 <sup>c</sup>	62.6			
[H <sub>1</sub> X <sub>2</sub> H <sub>3</sub> ...X <sub>4</sub> ] <sup>+</sup>						
2542.4	113.5	2719.7	202.3	3471.0	473.0	H <sub>1</sub> X <sub>2</sub> str.
921.0	1327.6	990.7	446.0	1342.2	166.5	H <sub>1</sub> X <sub>2</sub> H <sub>3</sub> bend.
808.8	4444.8	794.0	4327.9	2067.3	2254.3	X <sub>2</sub> H <sub>3</sub> X <sub>4</sub> str.
562.6	13.95	671.1	23.8	712.1	172.6	X <sub>2</sub> H <sub>3</sub> X <sub>4</sub> out of pl.
357.4	18.1	419.9	44.3	494.7	157.4	X <sub>2</sub> H <sub>3</sub> X <sub>4</sub> in pl.
200.7	64.8	251.5	167.9	326.3	68.9	H <sub>3</sub> X <sub>4</sub> str.
TS(H <sub>1</sub> X <sub>2</sub> ...H <sub>3</sub> X <sub>4</sub> ) (a Harmonic Spectrum)						
2636.7	147.0	2753.5	244.6			H <sub>1</sub> –X <sub>2</sub> str.
2017.9	410.5	2162.8	270.7			H <sub>3</sub> –X <sub>4</sub> str.
473.8	13.1	496.4	34.6			complicated
285.3	14.2	304.4	29.6			complicated
132.5	62.0	226.4	100.1			X <sub>2</sub> ...H <sub>4</sub> str.
-706.6	21.7	-791.0	30.9			

<sup>a</sup> HBrBrH tors + BrBr stretch. <sup>b</sup> ClCl stretch. <sup>c</sup> HClClH tors.

<sup>a</sup> HBrBrH tors + BrBr stretch. <sup>b</sup> ClCl stretch. <sup>c</sup> HCiClH tors.

are in good agreement with the experimental values. In the case of the [HCiClH]<sup>+</sup> complex, the calculated anharmonic frequencies of H–Cl stretching bands (2712.6 and 2709.4 cm<sup>-1</sup>) are in very good conformity with observed values (2704.1 and 2703.1 cm<sup>-1</sup>). The bands' intensities calculated for this complex suggest that the HCiCl asymmetric bending band is possible to observe at a frequency about 486 cm<sup>-1</sup>. There is a lack of experimental data confirming or rejecting this supposition, as the experiment was conducted in the range of 500–5000 cm<sup>-1</sup>.

As it was said, the authors of a previous experimental paper assigned tentatively two recorded absorptions to the stretching fundamentals of H<sub>2</sub>Cl<sup>+</sup> on the basis of similar frequencies recorded in the gas-phase experiment. Our calculations provide some arguments supporting this assignment. The lack of bending bands in the experimental spectrum could be explained by the fact that the calculated intensity of the band is an order of magnitude smaller than for the stretching ones. Apart from that, it could be possible that, upon irradiation, not only H<sub>2</sub>Cl<sup>+</sup> ions but also the [HCiH⋯Cl]<sup>+</sup> complex appeared in the deposit, which was not recognized by the authors of the previous experimental paper.

The irradiation process could cause the excitation, which would lead to H<sub>2</sub>Cl<sup>+</sup> or [HCiH⋯Cl]<sup>+</sup> products by similar mechanisms: [HCiClH]<sup>+</sup> → TS → H<sub>2</sub>Cl<sup>+</sup> or [HCiClH]<sup>+</sup> → TS → [HCiH⋯Cl]<sup>+</sup>. The calculated IR spectrum of the hydrogen-bonded complex suggests that the presence of the complex in the matrix upon irradiation should lead at least



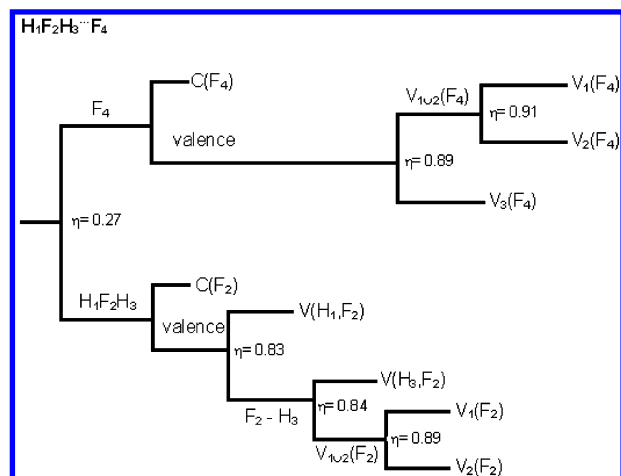


**Figure 2.** Localization domain reduction tree diagram of the  $[\text{H}_1\text{F}_2\text{H}_3\cdots\text{F}_4]^+$  complex.

to the band located at around  $793\text{ cm}^{-1}$  and connected with  $\text{ClHCl}$  stretching in the bridge, as this band is the most prominent in the spectrum of this complex, or even the band at around  $990\text{ cm}^{-1}$  originating from the  $\text{HClH}$  bending mode. Indeed, such bands were recorded, namely, weak absorption at  $752.0\text{ cm}^{-1}$  and very weak absorption at  $992.6\text{ cm}^{-1}$  originally attributed by the authors to the  $\text{ClHCl}^-$  ion. Both of the bands showed the same pattern of intensity change upon mercury-arc irradiation of the deposit as that of the bands originating from  $\text{H}_2\text{Cl}^+$  ion oscillations.

It is expected that anharmonic frequencies calculated for F-containing species would be in good agreement with the experimental values if they were accessible, as it is in the case of the Cl- and Br-type molecules.

Comparing calculated IR spectra of  $\text{H}_2\text{X}^+$  and hydrogen-bonded complexes, one can observe that for all complexes there is a strong red shift of the H-X stretching band as a result of complex formation (about  $1670\text{ cm}^{-1}$  for the Br-type molecule, about  $1840\text{ cm}^{-1}$  for the Cl complex, and about  $1270\text{ cm}^{-1}$  for the F-containing complex). Contrary to the typical hydrogen bonds, the red shift of  $\text{HXH}$  bending bands is observed as the result of complex formation.

**The Nature of Bonding in  $[\text{HXH}\cdots\text{X}]^+$  Complexes.** An interpretation of the ELF function used in this paper is based on the work of Becke and Edgecombe.<sup>15</sup> In this section, additional labeling of the atoms is used, unless it is not necessary for clarity.

The gradient field of the ELF function for the  $[\text{H}_1\text{X}_2\text{H}_3\cdots\text{X}_4]^+$  ( $\text{X} = \text{F}, \text{Cl}, \text{and Br}$ ) systems reveals attractors associated with the core electron density  $\text{C}(\text{X}_2)$  and  $\text{C}(\text{X}_4)$ , the nonbonding electron density  $\text{V}_{i=1,2}(\text{X}_2)$  and  $\text{V}_{i=1,3}(\text{X}_4)$ , and hydrogen-halogen bonds  $\text{V}(\text{H}_1, \text{X}_2)$  and  $\text{V}(\text{H}_3, \text{X}_2)$ . All valence attractors are of the point type.

The localization domain reduction tree diagrams of the  $[\text{H}_1\text{X}_2\text{H}_3\cdots\text{X}_4]^+$  complexes are presented in Figures 2–4, and a graphical representation of the localization domains and basins in an exemplary  $[\text{H}_1\text{Br}_2\text{H}_3\cdots\text{Br}_4]^+$  complex is presented in Figure 5. For  $\eta = 0.5$ , one can observe a large valence domain surrounding the whole complex. The  $\text{H}_1\text{Br}_2\text{H}_3$  and  $\text{Br}_4$  moieties are “stuck together” by the electron density with a noticeable degree of electron pairing. It confirms that the  $\text{H}_3\cdots\text{Br}_4$  region is dominated by covalent interactions. Upon going to the larger values of ELF (representation for  $\eta = 0.78$ ), the valence domain undergoes a splitting into three

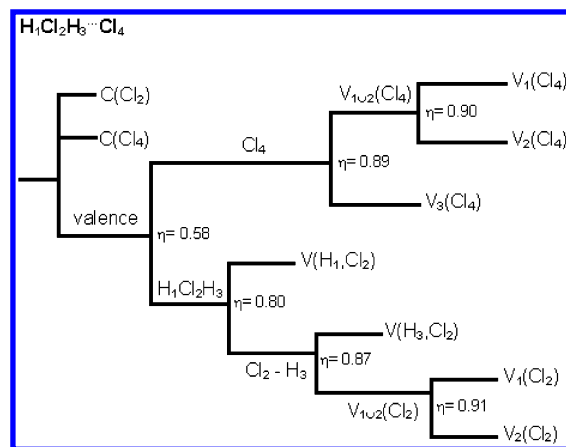


**Figure 3.** Localization domain reduction tree diagram of the  $[\text{H}_1\text{Cl}_2\text{H}_3\cdots\text{Cl}_4]^+$  complex.

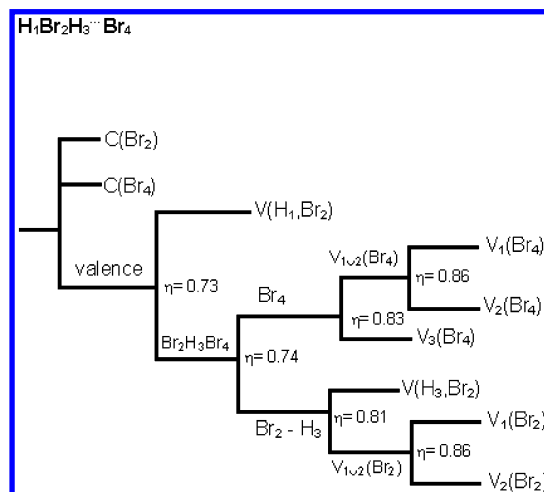


**Figure 4.** Localization domain reduction tree diagram of the  $[\text{H}_1\text{Br}_2\text{H}_3\cdots\text{Br}_4]^+$  complex.

smaller reducible domains. A representation for  $\eta = 0.83$  illustrates positions of attractors and associated localization basins. An interaction within the complex leads to a redistribution of the electron density from the  $\text{V}(\text{H}_3, \text{Br}_2)$  and  $\text{V}_3(\text{Br}_4)$  basins to  $\text{V}(\text{H}_1, \text{Br}_2)$  and  $\text{V}_1(\text{Br}_4) \cup \text{V}_2(\text{Br}_4)$  as revealed by the larger sizes of the latter ones.

All complexes can be described by approximate formulas— $[\text{HFH}]^{+0.93}\text{F}^{+0.07}$ ,  $[\text{HClH}]^{+0.86}\text{Cl}^{+0.15}$ , and  $[\text{HBrH}]^{+0.79}\text{Br}^{+0.22}$ —and a larger amount of the positive charge ( $q$ ) is concentrated on the  $\text{H}_1\text{X}_2\text{H}_3$  fragment. As one could expect, there is a gradual increase of  $q$  on the halogen going from F to Br in accordance with its growing polarizability. The very small charge ( $+0.07e$ ) found on  $\text{F}_4$  in  $[\text{HFH}\cdots\text{F}]^+$  supports the concept that the  $\text{F}_2\text{—H}_3\cdots\text{F}_4$  hydrogen bond possesses mainly electrostatic character.

A similar conclusion can be drawn using the core-valence bifurcation (CVB) index defined by Fuster and Silvi<sup>33</sup> as the difference of  $\eta(\mathbf{r}_{\text{CV}})$ , the lowest value of the ELF for which all the core basins of the complex are separated from the valence, and  $\eta(\mathbf{r}_{\text{AHB}})$ , the value at the saddle connection of the  $\text{V}(\text{A}, \text{H})$  and  $\text{V}(\text{B})$  basins  $\vartheta(\text{AHB}) = \eta(\mathbf{r}_{\text{CV}}) - \eta(\mathbf{r}_{\text{AHB}})$ . In the case of the  $[\text{H}_1\text{F}_2\text{H}_3\cdots\text{F}_4]^+$  complex, we estimated a value of  $\vartheta$  being about 0.17. An achieved positive value of  $\vartheta(\text{AHB})$  implies that the ELF topology of  $[\text{H}_1\text{F}_2\text{H}_3\cdots\text{F}_4]^+$  is just an addition of  $\text{H}_1\text{F}_2\text{H}_3$  and  $\text{F}_4$  moieties. Such a situation corresponds to the electrostatic interaction of  $\text{H}_1\text{F}_2\text{H}_3$  and

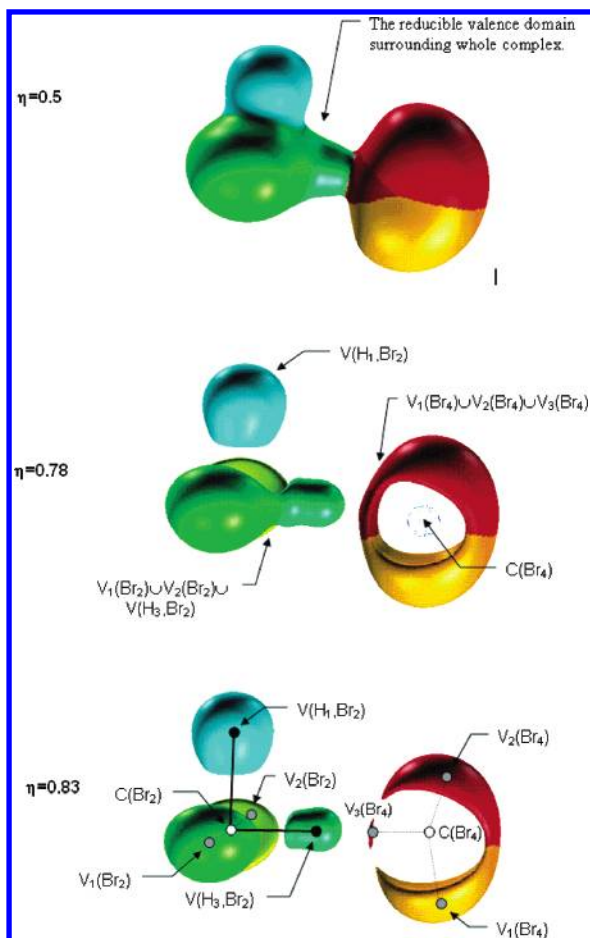


**Figure 5.** Reduction of localization domains in the  $[H_1Br_2H_3\cdots Br_4]^+$  complex. The solid lines correspond to the Lewis-type representation of bonding; the dashed lines connect valence attractors to atomic cores.

$F_4$ . For the  $[H_1Cl_2H_3\cdots Cl_4]^+$  and  $[H_1Br_2H_3\cdots Br_4]^+$  complexes, the values of the CVB index are negative:  $-0.30$  and  $-0.40$ , respectively. Both complexes can be viewed as single molecules since the core-valence separation occurs before the interacting subunits are isolated ( $\eta = 0.58$  and  $0.74$ ) and additional electron delocalization between HXH and X moieties occurs.<sup>33</sup>

Invented by Bader, the *Atoms in Molecules* method is a way of defining and classifying bonding interactions and is applicable also to supermolecules.<sup>34</sup> The bonds in the investigated systems have been characterized using bond critical point (bcp) parameters, namely, the charge density  $\rho_{bcp}$ , the Laplacian of charge density  $\Delta\rho_{bcp}$ , and ellipticity  $\epsilon$ . The AIM characterization of hydrogen bonds in  $[H_2X_2]^+$  structures is based on the criteria proposed by Popelier and Koch.<sup>35</sup> Apart from consistent topology, that is, the existence of a bcp for each hydrogen bond, a  $\rho_{bcp}$  value is expected to be within the range  $[0.002, 0.04]$  au, and  $\Delta\rho_{bcp}$  is in the range  $[0.02, 0.15]$  au.

AIM analyses of the bonding in the  $[H_1X_2H_3\cdots X_4]^+$  complexes provide results which are complementary and consistent with the conclusions from the ELF method. The  $X_2-H_3$  bond engaged in the hydrogen bridge is longer than the one in a free  $H_2X^+$  monomer, which is reflected in the parameters of the critical point of this bond. As it is seen from Table 5, complex formation decreases the value of electron density in bcp as well as the value of  $|\Delta\rho|$ , which

means that the covalent character of this bond decreases. As could be expected, the properties of the  $H_1-X_2$  bond remain almost unchanged. ELF analysis has revealed that the nature of the  $H_3\cdots X_4$  hydrogen bond depends strongly on the X atom and changes from the almost closed-shell type in the case of the F complex to the mostly covalent one in the Br-containing one. This conclusion finds full confirmation in light of the AIM analysis results. In the case of the  $H_3\cdots F_4$  bond, the value of  $\Delta\rho_c$  is positive; the bond is therefore of the closed-shell type, which is characteristic for the typical hydrogen bonds dominated by an electrostatic interaction; however, the value of  $\rho$  is larger than in typical cases. The complex with Br atoms (see Figures 6 and 7) has a hydrogen bond of the shared type, as the value of the Laplacian in bcp is negative. The character of the  $H_3\cdots Cl_4$  bond is intermediate as the value of  $\Delta\rho$  is close to zero. The fact that the stability of all  $[H_1X_2H_3\cdots X_4]^+$  complexes is similar is reflected in the similar values of electron density in hydrogen bonds' critical points, while the largest one is, as could be expected, for the most stable Br-containing complex.

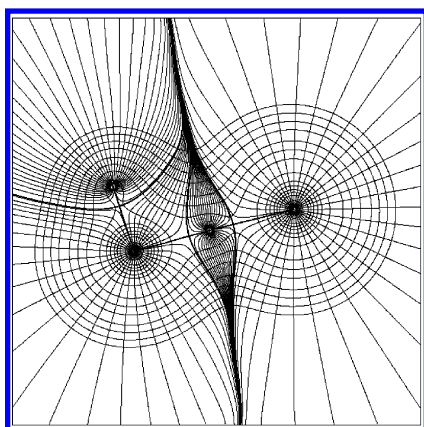
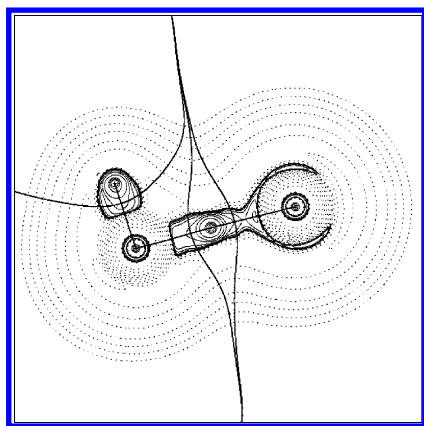
Integral data connected with Popelier's criteria of a hydrogen bond are collected in Table 6. They are obtained by subtracting appropriate values characterizing the hydrogen atom basin in the free  $H_2X^+$  monomer from the value obtained for the hydrogen atom in the complex. For comparison, the values both for the atom engaged in the  $X_2-H_3\cdots X_4$  bond and for the  $H_1$  one have been calculated and presented. Two of the criteria are the decrease of a hydrogen atom volume as well as its dipolar polarization upon hydrogen-bond formation. Table 6 shows that both mentioned criteria are fulfilled in the case of all three complexes. Changes of these parameters for the free  $H_1$  atom are evidently opposite of the ones for the  $H_3$  atom. Other criteria like the loss of the topological hydrogen atom charge and its energetic destabilization are fulfilled by the Br- and Cl-type complexes. In the case of the  $[HFH\cdots F]^+$  complex, changes of these integral parameters of the  $H_3$  atom are, surprisingly, opposite those expected and are similar to the ones for the non-hydrogen-bonded  $H_1$  atom.

**The Nature of Bonding in  $[HXXH]^+$  Complexes.** An analysis of a gradient field of the ELF function in the  $H_1X_2X_3H_4$  complexes presents two core attractors  $C(X_{i=2,3})$ , two monosynaptic attractors  $V_{i=1,2}(X)$  describing the non-bonding electron density of halogens  $X_2$  and  $X_3$ , and two protonated disynaptic attractors  $V(H_1, X_2)$  and  $V(H_4, X_3)$ . A schematic representation of attractors is shown in Figure 8 for  $\eta = 0.84$ , and localization domain reduction tree diagrams are presented in Figure 9. In both complexes, a separation between molecular domains of  $H_1X_2$  and  $X_3H_4$  occurs at much smaller ELF values ( $0.29$  and  $0.33$ ) than first valence bifurcation found for the  $[H_1X_2H_3\cdots X_4]^+$  ( $X = Cl, Br$ ) complexes ( $0.58$  and  $0.73$ ).

The formation of complexes from the isolated HX and  $HX^+$  molecules does not lead to a "creation" of new attractors; therefore, no essential redistribution of the electron density in monomers or an alteration of its electron localization properties is observed. We must emphasize that in the  $X_2\cdots X_3$  region a hypothetical  $V(X_2, X_4)$  attractor of the disynaptic type is missing; thus, the existence of a covalent  $X_2-X_3$  bond is ultimately excluded. According to a classification of interatomic interactions proposed by Silvi and

**Table 5.** Bond Critical Points Parameters

		HX	HX <sup>+</sup>	H <sub>2</sub> X <sup>+</sup>	[HXH...X] <sup>+</sup>			[HXXH] <sup>+</sup>		TS (HX...HX)		
		H-X	H-X	H-X	H-X	X-H	H...X	H-X	X-X	H-X	X...H	H-X
F	$\rho$	0.377	0.269	0.304	0.317	0.248	0.074					
	$\Delta\rho$	-3.231	-2.661	-3.031	-3.098	-1.877	0.150					
	$\epsilon$	0.000	0.018	0.009	0.007	0.010	0.040					
Cl	$\rho_c$	0.248	0.233	0.236	0.240	0.162	0.077	0.241	0.050	0.242	0.214	0.046
	$\Delta\rho$	-0.694	-0.754	-0.754	-0.738	-0.363	-0.005	-0.730	0.097	-0.714	-0.638	0.074
	$\epsilon$	0.000	0.059	0.051	0.038	0.043	0.053	0.037	0.030	0.014	0.040	0.182
Br	$\rho$	0.208	0.203	0.204	0.206	0.132	0.087	0.206	0.044	0.206	0.181	0.047
	$\Delta\rho$	-0.478	-0.559	-0.555	-0.530	-0.237	-0.073	-0.531	0.067	-0.513	-0.446	0.045
	$\epsilon$	0.000	0.062	0.057	0.035	0.045	0.048	0.038	0.017	0.014	0.034	0.181

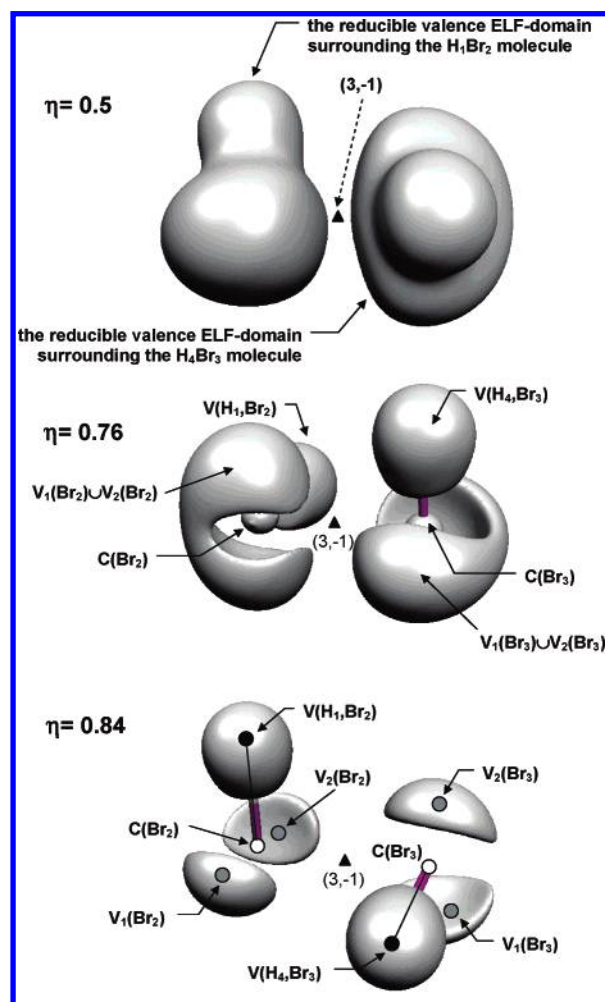
**Figure 6.** Contour map of the electron density in the [HBrH...Br]<sup>+</sup> complex superimposed on the gradient vector field in the symmetry plane.**Figure 7.** Contour map of the Laplacian density in the [HBrH...Br]<sup>+</sup> complex as well as the interatomic surfaces in the molecular plane. Dashed lines represent positive values of  $\Delta\rho$ , full lines, negative ones.

Savin,<sup>16</sup> the X<sub>2</sub>...X<sub>3</sub> binding belongs to the closed-shell electron interaction type.

This picture is supported by the results of an AIM analysis, which are collected in Table 5. Because of the positive value of  $\Delta\rho_{\text{bcp}}$ , the X<sub>2</sub>-X<sub>3</sub> bond is definitely of the closed-shell type (Figures 10 and 11). The values of  $\rho_{\text{bcp}}$  for these bonds are small, even smaller than the value for the hydrogen bonds in the [H<sub>1</sub>X<sub>2</sub>H<sub>3</sub>...X<sub>4</sub>]<sup>+</sup> complexes. The closed-shell character of the interaction together with the lack of electron density at the critical point of the X<sub>2</sub>-X<sub>3</sub> bond could suggest that the [H<sub>1</sub>X<sub>2</sub>H<sub>3</sub>...X<sub>4</sub>]<sup>+</sup> structures are weakly bonded. The results of ab initio calculations discussed at the beginning of this article unanimously pointed out that these complexes are much more stable than could be expected on the basis of topological AIM and ELF considerations. The formation of

**Table 6.** Integral Properties of the Hydrogen Atoms in [HXH...X]<sup>+</sup> Hydrogen-bonded Systems

	[H <sub>1</sub> F <sub>2</sub> H <sub>3</sub> ...F <sub>4</sub> ] <sup>+</sup>		[H <sub>1</sub> Cl <sub>2</sub> H <sub>3</sub> ...Cl <sub>4</sub> ] <sup>+</sup>		[H <sub>1</sub> Br <sub>2</sub> H <sub>3</sub> ...Br <sub>4</sub> ] <sup>+</sup>	
	H <sub>1</sub>	H <sub>3</sub>	H <sub>1</sub>	H <sub>3</sub>	H <sub>1</sub>	H <sub>3</sub>
$N(\Omega)$	0.163	0.149	0.651	0.544	0.770	0.641
$\Delta N(\Omega)$	0.012	0.043	0.044	-0.063	0.051	-0.078
$E(\Omega)$	-0.188	-0.204	-0.455	-0.369	-0.484	-0.396
$\Delta E(\Omega)$	-0.012	-0.028	-0.025	0.061	-0.027	0.061
$V(\Omega)$	9.149	5.678	32.722	19.938	40.243	24.445
$\Delta V(\Omega)$	0.592	-2.870	2.223	-10.561	2.953	-12.845
$M(\Omega)$	0.069	0.049	0.084	0.035	0.063	0.022
$\Delta M(\Omega)$	0.007	-0.013	0.008	-0.041	0.008	-0.033

**Figure 8.** Reduction of localization domains in the [H<sub>1</sub>Br<sub>2</sub>...Br<sub>3</sub>H<sub>4</sub>]<sup>+</sup> complex.

these structures from the natural monomers is thermodynamically profitable, and dissociation energy (defined as  $E_{\text{tot,ZPE}}([HXXH])^+ - E_{\text{tot,ZPE}}(\text{HX}) - E_{\text{tot,ZPE}}(\text{HX}^+)$ ) is about



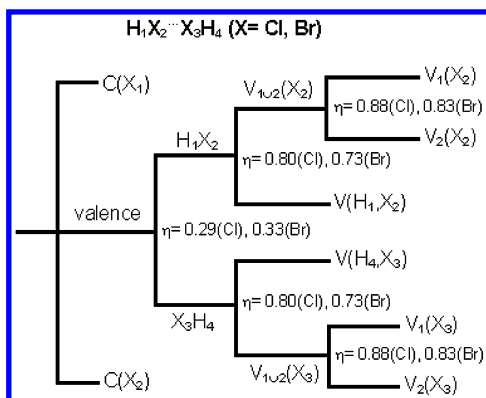


**Figure 9.** Localization domain reduction tree diagram of the  $[H_1X_2\cdots X_3H_4]^+$  complex ( $X = \text{Br}, \text{Cl}$ ).

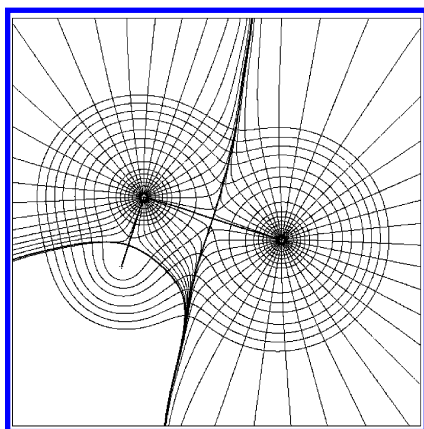


**Figure 10.** Contour map of the electron density in the  $[HBrBrH]^+$  complex superimposed on the gradient vector field in a HBrBr plane. For clarity, the vector field only in the Br atoms' basins is shown.

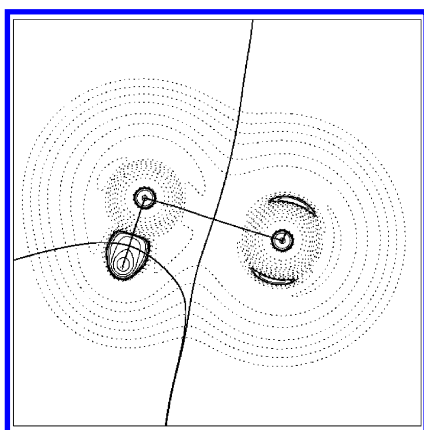


**Figure 11.** Contour map of the Laplacian density in the  $[HBrBrH]^+$  complex as well as the interatomic surfaces in a HBrBr plane.

$-30.5 \text{ kcal mol}^{-1}$  for both Cl- and Br-type molecules, which is more than half of the binding energy of  $\text{Cl}_2$  or  $\text{Br}_2$  molecules. Thermodynamics support, therefore, a thesis that the structures arise due to a half-occupied covalent  $X_2-X_3$  bond.

This seeming discrepancy could be explained if the open-shell electron structure of the complexes and its essential influence on the electron pairing in the complexes is considered. According to the Hellmann–Feynman electrostatic theorem, the forces acting on a nucleus in a molecule are the sum of electrostatic ones exerted by the other nuclei and by a hypothetical electron cloud whose charge density

is given by the solutions of the electronic Schrödinger equation. The values of dissociation energy clearly show that in spite of the lack of electron density in the  $X_2-X_3$  space there is enough “glue” which very effectively “sticks together”  $[\text{HX}]^{+0.5}$  moieties. The nature of the  $X_2-X_3$  bond seems to be similar to the covalent-depleted ones in molecules like  $\text{F}_2^{36}$  or  $\text{HOO}^{37}$  where electrons are “pushed” from the F–F or O–O bond region and strongly localized in atomic basins.

The NBO method localizes a singly occupied bonding orbital (say,  $\beta$ ) connected with an  $X_2-X_3$  bond and two singly occupied  $\alpha$  orbitals connected with “lone electrons”—one per each X atom. The  $\beta$  electron is a possible candidate to be paired with one of the free  $\alpha$  electrons. Symmetry of the complex requires the same level of pairing with both  $\alpha$  electrons, which have to avoid each other according to the Pauli rule. As a result, an effective pairing between the  $\beta$  electron and  $\alpha$  electrons takes place in the vicinity of X atoms rather than in a midpoint of the  $X_2-X_3$  bond, which manifests in a decrease of electron density at the bond critical point and a small value of the ELF field in this area.

A reduction of localization basins for an exemplary  $[H_1\text{Br}_2\cdots\text{Br}_3H_4]^+$  complex is presented in Figure 8, where some differences in respect to the  $[H_1\text{Br}_2H_3\cdots\text{Br}_4]^+$  system may be noticed. First of all, a splitting of a valence-reducible domain surrounding the whole system (representation for  $\eta = 0.5$ ) yields two smaller domains containing the  $H_1\text{Br}_2$  and  $H_4\text{Br}_3$  monomers. A bifurcation occurs for an ELF value equal to 0.33 ( $\eta_{\text{Cl}} = 0.29$ ), being about 2 times smaller than that observed in  $[H_1\text{Br}_2H_3\cdots\text{Br}_4]^+$ . Furthermore, a difference between  $\eta_{\text{Cl}}$  and  $\eta_{\text{Br}}$  is very small (0.04) as compared to the rather large (0.15) change observed for  $[H_1X_2H_3\cdots X_4]^+$  ( $X = \text{Cl}, \text{Br}$ ). This finding agrees well with the closed-shell type of  $X_2\cdots X_3$  interaction where a lack of the electron density is reflected by a small alteration in the degree of electron localization. For  $\eta = 0.78$ , the localization basins of the  $H_1-\text{Br}_2$  and  $H_4-\text{Br}_3$  bonds are well-isolated and the nonbonding electron density of the Br atoms is described by two large  $V_1(\text{Br}_2) \cup V_2(\text{Br}_2)$  and  $V_1(\text{Br}_3) \cup V_2(\text{Br}_3)$  domains. A representation for  $\eta = 0.84$  presents all attractor basins separated.

**Transition Structure.** An analysis of the ELF function carried out for transition state structures  $[H_1X_2\cdots H_3X_4]^+$  reveals a picture of two H–X monomers where valence shells of halogens are characterized by two monosynaptic basins.

In the case of molecules that are not in a local minimum on the PES, it is formally not possible to define a chemical bond in a sense of AIM theory. However, the properties of the interaction between subsystems in the analyzed structures could be somehow characterized using parameters of the (3,  $-1$ ) critical points on the interatomic lines connecting the appropriate atoms, namely,  $H_3$  and  $X_2$  ones (Figure 1). In both complexes, the Laplacian at the critical point is positive and the value of electron density is small. The large value of the ellipticity points at the topological instability of the structures.

## FINAL REMARKS

The H–X bonds in a series of molecules—HX,  $H_1-X_2$  in the TS structure,  $H_1-X_2$  in the  $[H_1X_2H_3\cdots X_4]^+$  system, and



H–X in  $\text{H}_2\text{X}^+$ —correspond to the steps in a formal process of a proton transfer between the HX molecule and the  $\text{HX}^+$  ion. In these moieties, the H atom is free (i.e., not engaged in hydrogen-bond formation) and the X atom is more and more strongly engaged in creation of a bond with another hydrogen atom. For these H–X moieties, an increase of the bond length, decrease of the electron density at the bcp, decrease of  $\Delta\rho_{\text{bcp}}$ , and increase of ellipticity are observed. Similar relationships are observed in a set of H–X bonds in H–X,  $[\text{HXXH}]^+$ , and  $\text{HX}^+$  molecules. Not only parameters of bond critical points but also H–X stretching frequencies should correlate with the bond length.

For all these H–X bonds, the bond length exhibits more or less a linear correlation with the above-mentioned parameters, while the linear dependence is the most evident in the case of Cl-type molecules. For example, for these structures, the calculated harmonic H–Cl frequency depends on the bond length as follows:  $\nu(r) = -8155.9r + 13345$ , where the  $R^2$  factor is 0.9992. In the case of anharmonic frequency and the value of  $\rho_{\text{bcp}}$ , the value of  $R^2$  is 0.9982 and 0.9921, respectively. In the case of F- and Br-containing structures, the linear dependence is slightly worse.

## CONCLUSIONS

On the potential energy surface of the  $[\text{H}_2\text{X}_2]^+$  complexes containing Br or Cl atoms, there are two local minima referring to the  $[\text{HXH}\cdots\text{X}]^+$  hydrogen-bonded structure and to the most stable  $[\text{HX}-\text{XH}]^+$  three-electron-bonded one. This conclusion is the same as in the previously published papers devoted to this issue. Contrary to the previous results, we claim that for the F-containing complex the only possible stable structure is the hydrogen-bonded one. The three-electron-bonded complex reported in previous papers should be considered as an artifact as it is described by an unstable wave function.

Calculated harmonic and anharmonic IR spectra enabled a deeper analysis of the results obtained by Jacox et al. in the low-temperature matrix experiment and confirmed that the  $[\text{HBrBrH}]^+$  and  $[\text{HClClH}]^+$  complexes were observed. Moreover, we suggest that some frequencies, which were observed after mercury-arc irradiation, assigned to the  $\text{ClHCl}^-$  ion could originate from the hydrogen-bonded  $[\text{HClH}\cdots\text{Cl}]^+$  form.

Stability of the hydrogen-bonded complexes as well as the nature of the hydrogen bond depends on the halogen atoms. The most stable complex is the Br-containing one, and the least stable is the F-type one. Topological AIM and ELF methods revealed that the hydrogen bond in the  $[\text{HBrH}\cdots\text{Br}]^+$  complex is mostly covalent, whereas the bond in the F-containing structure is ultimately of the closed-shell type. All these complexes are an important example of the structures containing a hydrogen bond which does not fulfill criteria proposed by Popelier.

The X–X three-electron two-center bonds in the three-electron-bonded structures are of the closed-shell type. The bonds are much stronger, however, than could be expected on the basis of a very low value of electron density at the bond critical point. This phenomenon can be explained considering the radical electron structure and symmetry of the complexes. The nature of these bonds is similar to the covalent-depleted bonds in  $\text{F}_2$  or  $\text{HOO}$  molecules, but the

effect of removing electrons from the bond area is much stronger.

## ACKNOWLEDGMENT

The authors thank the Wrocław Supercomputer and Networking Center for a computer time grant.

## REFERENCES AND NOTES

- (1) Jeffrey, G. A. *An Introduction to Hydrogen Bonding*; Oxford University Press: New York, 1997.
- (2) Gill, P. M. W.; Radom, L. Structures and Stability of Singly Charged Three-Electron Hemibonded Systems and Their Hydrogen-Bonded Isomers. *J. Am. Chem. Soc.* **1988**, *110*, 4931–4941.
- (3) Clark, T. Odd-Electron  $\sigma$  Bonds. *J. Am. Chem. Soc.* **1988**, *110*, 1672–1678.
- (4) Burda, J. V.; Hobza, P.; Zahradnik, R. Properties and Reactivity in Groups of the Periodic System: Ion–Molecule Reactions  $\text{HX} + \text{HX}^{*+}$  (X = F, Cl, Br, I, At). *J. Phys. Chem. A* **1997**, *101*, 1134–1139.
- (5) Hiberty, P. C.; Humber, S.; Archirel, P. Nature of the Differential Electron Correlation in Three-Electron Bond Dissociations. Efficiency of a Simple Two-Configuration Valence Bond Method with Breathing Orbitals. *J. Phys. Chem.* **1994**, *98*, 11697–11704.
- (6) Sodupe, M.; Oliva, A.; Bertran, J. Theoretical Study of the Ionization of the  $\text{H}_2\text{O}-\text{H}_2\text{O}$ ,  $\text{NH}_3-\text{H}_2\text{O}$ ,  $\text{FH}-\text{H}_2\text{O}$  Hydrogen Bonded Molecules. *J. Am. Chem. Soc.* **1994**, *116*, 8249–8258.
- (7) Sodupe, M.; Oliva, A.; Bertran, J. Theoretical Study of the Ionization of the  $\text{H}_2\text{S}-\text{H}_2\text{S}$ ,  $\text{PH}_3-\text{H}_2\text{S}$ ,  $\text{ClH}-\text{H}_2\text{S}$  Hydrogen Bonded Molecules. *J. Am. Chem. Soc.* **1995**, *117*, 8416–8421.
- (8) Harcourt, R. D. Valence Bond and Molecular Orbital Descriptions of the Three-Electron Bond. *J. Phys. Chem. A* **1997**, *101*, 2496–2501.
- (9) Bickelhaupt, F. M.; Diefgenbach, A.; de Visser, S. P.; de Koning, L. J.; Nibbering, N. M. M. Nature of the Three-Electron Bond in  $\text{H}_2\text{S}-\text{SH}_2^+$ . *J. Phys. Chem. A* **1998**, *102*, 9549–9553.
- (10) Sodupe, M.; Bertran, J.; Rodriguez-Santiago, L.; Baerends, E. J. Ground State of the  $(\text{H}_2\text{O})_2^+$  Radical Cation: DFT versus Post-Hartree–Fock Methods. *J. Phys. Chem. A* **1999**, *103*, 166–170.
- (11) Uchimaru, T.; Tsuzuki, S.; Sugie, M.; Tokuhashi, K.; Sekiya, A. A Theoretical Study on the Strength of Two-Center Three-Electron Bond in  $(\text{CH}_3)_2\text{S}-\text{OH}$  and  $\text{H}_2\text{S}-\text{OH}$  Adducts. *Chem. Phys. Lett.* **2005**, *408*, 216–220.
- (12) Forney, D.; Jacox, M. E.; Thompson, W. E. The Vibrational Spectra of Molecular Ions Isolated in Solid Neon. XII.  $\text{HCl}^+$ ,  $(\text{HCl})_2^+$ ,  $\text{ClHCl}^-$ , and  $\text{O}_2\cdots\text{HCl}^+$ . *J. Chem. Phys.* **1995**, *103*, 1755–1766.
- (13) Lugez, C. L.; Jacox, M. E.; Thompson, W. E. The Vibrational Spectra of Molecular Ions Isolated in Solid Neon. XIII. Ions Derived from HBr and HI. *J. Chem. Phys.* **1996**, *105*, 3901–3910.
- (14) Bader, R. F. W. *Atoms in Molecules: A Quantum Theory*; Oxford University Press: Oxford, U. K., 1994.
- (15) Becke, A. D.; Edgecombe, K. E. A Simple Measure of Electron Localization in Atomic and Molecular Systems. *J. Chem. Phys.* **1990**, *92*, 5397–5403.
- (16) Silvi, B.; Savin, A. Classification of Chemical Bonds Based on Topological Analysis of Electron Localization Functions. *Nature* **1994**, *371*, 683–686.
- (17) Reed, A. E.; Curtiss, L. A.; Weinhold, F. Intermolecular Interactions from Natural Bond Orbital, Donor–Acceptor Viewpoint. *Chem. Rev.* **1988**, *88*, 899–926.
- (18) Perrin, C. L. Atomic Size Dependence of Bader Electron Populations: Significance for Questions of Resonance Stabilization. *J. Am. Chem. Soc.* **1991**, *113*, 2865–2868.
- (19) Poater, J.; Sola, M.; Bickelhaupt, F. M. Hydrogen–Hydrogen Bonding in Planar Biphenyl, Predicted by Atoms-In-Molecules Theory, Does Not Exist. *Chem.–Eur. J.* **2006**, *12*, 2889–2895.
- (20) Bader, R. F. W. Pauli Repulsions Exist Only in the Eye of the Beholder. *Chem.–Eur. J.* **2006**, *12*, 2896–2901.
- (21) Poater, J.; Sola, M.; Bickelhaupt, F. M. A Model of the Chemical Bond must be Rooted in Quantum Mechanics, Provide Insight, and Possess Predictive Power. *Chem.–Eur. J.* **2006**, *12*, 2902–2905.
- (22) Möller, C.; Plesset, M. S. Note on an Approximation Treatment for Many-Electron Systems. *Phys. Rev.* **1934**, *46*, 618–622.
- (23) Krishnan, R.; Binkley, J. S.; Seeger, R.; Pople, J. A. Self-Consistent Molecular Orbital Methods. XX. A Basis Set for Correlated Wave Functions. *J. Chem. Phys.* **1980**, *72*, 650–654.
- (24) McLean, A. D.; Chandler, G. S. Contracted Gaussian Basis Sets for Molecular Calculations I. Second Row Atoms,  $Z=11-18$ . *J. Chem. Phys.* **1980**, *72*, 5639–5648.
- (25) Frisch, M. J.; Pople, J. A.; Binkley, J. S. Self-Consistent Molecular Orbital Methods 25. Supplementary Functions for Gaussian Basis Sets. *J. Chem. Phys.* **1984**, *80*, 3265–3269.

- (26) Popelier, P. L. A.; Burke, J.; Malcolm, N. O. J. Functional Groups Expressed as Graphs Extracted from the Laplacian of the Electron Density. *Int. J. Quantum Chem.* **2003**, *92*, 326–336.
- (27) Frisch, M. J.; Trucks, G. W.; Schlegel, H. B.; Scuseria, G. E.; Robb, M. A.; Cheeseman, J. R.; Montgomery, J. A., Jr.; Vreven, T.; Kudin, K. N.; Burant, J. C.; Millam, J. M.; Iyengar, S. S.; Tomasi, J.; Barone, V.; Mennucci, B.; Cossi, M.; Scalmani, G.; Rega, N.; Petersson, G. A.; Nakatsuji, H.; Hada, M.; Ehara, M.; Toyota, K.; Fukuda, R.; Hasegawa, J.; Ishida, M.; Nakajima, T.; Honda, Y.; Kitao, O.; Nakai, H.; Klene, M.; Li, X.; Knox, J. E.; Hratchian, H. P.; Cross, J. B.; Bakken, V.; Adamo, C.; Jaramillo, J.; Gomperts, R.; Stratmann, R. E.; Yazyev, O.; Austin, A. J.; Cammi, R.; Pomelli, C.; Ochterski, J. W.; Ayala, P. Y.; Morokuma, K.; Voth, G. A.; Salvador, P.; Dannenberg, J. J.; Zakrzewski, V. G.; Dapprich, S.; Daniels, A. D.; Strain, M. C.; Farkas, O.; Malick, D. K.; Rabuck, A. D.; Raghavachari, K.; Foresman, J. B.; Ortiz, J. V.; Cui, Q.; Baboul, A. G.; Clifford, S.; Cioslowski, J.; Stefanov, B. B.; Liu, G.; Liashenko, A.; Piskorz, P.; Komaromi, I.; Martin, R. L.; Fox, D. J.; Keith, T.; Al-Laham, M. A.; Peng, C. Y.; Nanayakkara, A.; Challacombe, M.; Gill, P. M. W.; Johnson, B.; Chen, W.; Wong, M. W.; Gonzalez, C.; Pople, J. A. *Gaussian 03*, revision C.02; Gaussian, Inc.: Wallingford, CT, 2004.
- (28) Schmidt, M. W.; Baldridge, K. K.; Boatz, J. A.; Elbert, S. T.; Gordon, M. S.; Jensen, J. H.; Koseki, S.; Matsunaga, N.; Nguyen, K. A.; Su, S. J.; Windus, T. L.; Dupuis, M.; Montgomery, J. A. General Atomic and Molecular Electronic Structure System. *J. Comput. Chem.* **1993**, *14*, 1347–1363.
- (29) Biegler-König, F. W.; Bader, R. W. F.; Tang, T.-H. Calculation of the Average Properties of Atoms in Molecules. II. *J. Comput. Chem.* **1982**, *3*, 371–328.
- (30) Noury, S.; Krokidis, X.; Fuster, F.; Silvi, B. Computational Tools for Electron Localization Function Topological Analysis. *Comput. Chem.* **1999**, *23*, 597–604.
- (31) Pepke, E.; Murray, J.; Lyons, J.; Hwu, Y.-Z. *Scian*; Supercomputer Computations Research Institute, Florida State University: Tallahassee, FL, 1993.
- (32) Tiedemann, P. W.; Anderson, S. L.; Ceyer, S. T.; Hirooka, T.; Ng, C. Y.; Mahan, B. H.; Lee, Y. T. Proton Affinities of Hydrogen Halides Determined by the Molecular Beam Photoionization Method. *J. Chem. Phys.* **1979**, *71*, 605–609.
- (33) Fuster, F.; Silvi, B. Does the Topological Approach Characterize the Hydrogen Bond? *Theor. Chem. Acc.* **2000**, *104*, 13–21.
- (34) Bader, R. W. F. A Bond Path: A Universal Indicator of Bonded Interactions. *J. Phys. Chem. A* **1998**, *102*, 7314–7323.
- (35) Koch, U.; Popelier, P. L. A. Characterization of C–H–O Hydrogen Bonds on the Basis of the Charge Density. *J. Phys. Chem.* **1995**, *99*, 9747–9754.
- (36) Llusa, R.; Beltran, A.; Andres, J.; Noury, S.; Silvi, B. Topological Analysis of Electron Density in Depleted Homopolar Chemical Bonds. *J. Comput. Chem.* **1999**, *20*, 1517–1526.
- (37) Bil, A.; Latajka, Z. The Examination of the Hydroperoxy Radical and Its Closed-Schell “Analogues” by Means of Topological Methods of Quantum Chemistry: AIM and ELF. *Chem. Phys.* **2004**, *303*, 43–53.

CI600355G